# Auger Transition Spectra Through De-excitation Decay of Inner-Shell Vacancy in Atom

**Adel Mohammedein El-Shemi**
**Applied Sciences Department, College of Technological Studies**
**P.O. Box 42325, Shuwaikh 70654, Kuwait**
**E-mail: admohamed@yahoo.com**

**Abstract**

The relaxation of core hole in atom via parallel Auger cascades leads to the production of highly charged ions. During Auger cascade development, several Auger satellite spectra arise from the presence of spectator vacancies in the electronic configurations. The production of spectator vacancies after each Auger transitions cause characteristic energy shifts and more multiplet splitting. The change of Auger transition energies and transition rates, which arises from the presence of multi-vacancies in the configuration, is calculated for Ne and Ar after K-shell ionization. The shift of the transition energy depends on the spectator vacancy distributions in the configurations. The change of transition energies in course of cascade development may close some low-energy Auger channels. The consideration of these forbidden Auger transitions in the calculation of highly charged ions leads to results agree well with experimental values.

## Introduction

The de-excitation decays of a core-ionized atom via parallel cascades of radiative and Auger transitions generate different ionic charged ions. The relaxation of inner-shell ionized atom leads to emission of Auger spectra. In the course of the de-excitation decay pathway, multiple vacancies are generated after each Auger transitions. The distribution of these vacancies is independent of the initial ionization process. The Auger spectra that appearing in the course of de-excitation pathway arise from spectator vacancies left by preceding Auger transitions, from shake process accompanying the Auger transitions and from doubly ionized states created in the primary collision. All subsequence transitions of the de-excitation cascade occur in the presence of additional vacancies lift by the preceding transitions. The vacancy cascades correspond to transitions with emission of photon spectra or electron spectra for each branch in the vacancy cascade trees. Thereby, Auger spectra arise from the transitions between a various configurations with additional spectator vacancies

through the de-excitation cascades. The Auger spectra are conditioned by the transition rates and transition energies of multi-vacancy states. The presence of the additional vacancies leads to congested spectrum during the de-excitation decays. The reason for observing this congested spectrum is the presence of several open shells in the initial as well as final states. The generation of vacancies in the course of de-excitation cascade is accompanied by shift of energy levels. The influence of the additional vacancies during the cascades may close some Auger channels (forbidden energies). The overlapping spectra emitted on parallel branches of the de-excitation cascades lead to different final charge state of ions. The understanding of the influence of the spectator vacancies during the cascade development on the Auger transitions gives more detailed information about the process that appear after the core ionization.

The study of the radiative and Auger transition spectra for atom with multi-vacancy configurations is of particular interest in plasma physics[1], and for the decomposition of large molecules following electron pick-up [2].

The Auger transition rates and transition energies in multi-ionized neon atom are measured using heavy-ion and electron bombardment [3], and calculated using Hartree-Fock-Slater wave functions [4]. The influence of multi-vacancy states on the electron binding energies and transition rates in K, L, and M subshell are investigated in the calculation of ion charge state distributions [5,6]. The Auger and x-ray spectra that formed during vacancy cascades are calculated using Monte Carlo method [7,8]. The transition energies are obtained by Hartree-Fock-Pauli approximation. The change of Auger transition rates and the closing of Auger channels with forbidden energies are included in the calculation of ion charge state distributions, which produced after inner-shell ionization [9,10,11]. The $L_{23}MM$ spectra of argon excited at energies between those of K- and L- thresholds and affected by $L_1L_{23}M$ intermediate transition were measured and calculated [12]. The $L_{23}MM$ Auger spectra of argon emitted after photoexcitation were measured using broad-band synchrotron radiation of energies largely lying above the K- shell ionization potential [13]. Auger spectra of Na, Mg and Ar emitted after K-ionization were calculated by Omar and Hahn [14].

In the present work, the Auger spectra formed during vacancy cascade are calculated for Ne and Ar atoms. The Auger transition rates and transition energies are obtained using Dirac- Fock -Slater [15]. The influence of multi- vacancy that created

through de-excitation cascades is considered in the calculation. The forbidden Auger channels due to the shift of binding energy levels are presented for L- Auger transitions. The Auger transition energy shifts in Ne and Ar atoms with several vacancies in the electronic configurations are calculated in the present work. Finally, the highly charged ions for Ar with K-shell ionization are compared with experimental values.

## 2. Method of calculation

The ionized atom that remains after the ejected of the core hole electron is in a highly excited state and will rapidly relax back to a lower energy state by one of two processes:

i) Radiative process (x-ray fluorescence), or

ii) Non-radiative process (Auger emission)

The production of core hole in the target atom A is performed by photoionization $h\nu$

$$A + h\nu \rightarrow A^{+} + e_{p} \quad (1)$$

where $A^{+}$ is the atom in highly excited state, $e_p$ is the primary emitted electron. In the case of radiative process, the vacancy transfers to a higher shell under emission of characteristic x-rays

$$A^{+} \rightarrow A^{1+} + h\nu' \quad (2)$$

If the vacancy is filled via Auger emission resulting two vacancies in the higher shells in atom

$$A^{+} \rightarrow A^{2+} + e_{Auger} \quad (3)$$

where $A^{2+}$ is doubly ionized atom.

In this case, one electron falls from a higher level to fill an initial core hole and the energy liberated in this process in simultaneously transferred to a second electron; a fraction of this energy is required to overcome the binding energy of this second electron, the remainder is retained by this emitted Auger electron as kinetic energy of this second electron. In the Auger process, the final state is a doubly-ionized atom with core hole in the higher subshell. Theses new vacancies could be transferred into the ground state via a cascade of successive radiative and Auger processes. These sequent processes lead to highly charged ions.

The kinetic energy of the Auger electron can estimate from the binding energies of the various levels involved in the transition.

$E_{Kin}$=E (initial vacancy)- E (state of elect. filling hole)- E(state of elect. leaving) (4)

As an example: if K-shell vacancy filled by electron leaving $L_I$, with electron from $L_{II,III}$ leaving:

$$E_{Kin} = E_K - (E_{L_I} + E_{L_{II,III}}) \tag{5}$$

This type of transition is referred to in general as a $KL_I$ $L_{II,III}$ transition. If the first two letters are same, the transition is called Coster-Kronig transition.

The highly charged ions that produce after successive radiative and Auger processes in Ne and Ar atom are calculated. The calculation method is based on the simulation of all possible radiative and non-radiative pathways to fill the inner-shell vacancies in the atom. The calculation technique is used for simulating de-excitation cascade decays following inner-shell vacancy creation, considering fluorescence yields (radiative branching ratios), Auger and Coster-Kronig yields (non-radiative branching ratios), and electron shake-off processes. The radiative and non-radiative branching ratio is defined as the probability that the vacancy in an atom is filled through x-ray transitions (photon emission) or through Auger and Coster-Kronig processes, respectively. They are calculated as follows:

fluorescence yield

$$\omega(f \to i) = \frac{\Gamma_{if}^{R}}{\Gamma} \tag{6}$$

and Auger yield

$$a(f \to i) = \frac{\Gamma_{if}^{A}}{\Gamma} \tag{7}$$

Here, the initial configuration is given by i decaying into the final configuration f. $\Gamma$ is the sum of partial radiative widths $\Gamma_{if}^{R}$ and non-radiative width $\Gamma_{if}^{A}$, given by

$$\Gamma = \sum_{i,f} \Gamma_{if}^{R} + \sum_{i,f} \Gamma_{if}^{A} \tag{8}$$

The partial widths for radiative decay in a singly ionized atom are calculated (in atomic unit) as follows:

$$\Gamma_{if}^{R}(f \to i) = (4/3)(\Delta E/c)^3 \left| \langle \Psi_f | D | \Psi_i \rangle \right|^2 \tag{9}$$

where $\Psi_i$ and $\Psi_f$ are the initial and final states of the system, respectively. $\Delta E$ is the energy difference between these states, c is the speed of light. D is the electric dipole operator.

The non-radiative partial widths are obtained as:

$$\Gamma_{if}^{A}(f \to i) = \frac{2\pi}{\hbar} \bar{\sum} \left| \left\langle \Psi_f \left| H^{ee} \right| \Psi_i \right\rangle \right|^2 \rho(\varepsilon) \qquad (10)$$

where $H^{ee}$ is the operator of the electron-electron interaction. The density of final state $\rho(\varepsilon)$ is unity when the continuum-state wave function is normalized in the energy scale. The $\bar{\sum}$ denote the average and the sum over the initial and the final states, respectively.

The calculations of radiative transition rates were performed for singly ionized atoms using Multiconfiguration-Dirac-Fock (MCDF) wave functions [16]. The non-radiative transition rates were computed using Dirac-Fock-Slater (DFS) wave functions [15].

**3. Results and Discussions**

The creation of multiple vacancies in atomic configurations during vacancy population causes transition energy shifts and may result in an energetic closing of channels for certain Auger channels. The K-$L_{23}L_{23}$ and K-$L_1L_{23}$ Auger energy shifts for multi-ionized neon atom with configuration $1s^1\ 2s^2\ 2p^{6-n}$, where n ranged from 0 to 6 vacancies, are shown in Figure1. The energy shifts are calculated between normal Auger transition energy of configuration $1s^1\ 2s^2\ 2p^6$ and non-diagram Auger transition energies in configuration $1s^1\ 2s^2\ 2p^{6-n}$. The energies of Auger transitions decrease with increase the number of vacancies in the electronic configurations. It is common for all transitions, that the ionization of electrons from subshells causes a clear change in the transition energies. This behaviour is connected with the reduced screening of the remaining electrons in the atomic configurations. In highly ionized atoms the nuclear attraction dominates sufficiently against the electron-electron repulsion, so that all nl- electrons are more tightly bound than any (n+1)l electrons. The results are compared with values calculated by Hartree- Fock-Slater atomic model [4].

Because most Coster–Kronig energies are so low and the rates are so sensitive to the transition energy, some Auger channels may be energetically forbidden during the cascade de-excitation decays. The production of various vacancies in intermediate

configurations during the cascade decay is due to a closing of the Coster-Kronig channels. Table 1 gives the closing of Auger channels with forbidden energies during the cascade development. The Auger transition energies are calculated by using equation 4. The multi-vacancy configurations of Ar generate in the course of de-excitation decay followed K shell ionization. The prohibition of the highest-energy Auger transitions in the configuration $1s^2\ 2s^2\ 2p^{6-i}\ 3s^{2-j}\ 3p^{6-k}$ is as shown E (eV)<0, where i, j, and k indicate the number of vacancies.

Table 1: The Auger transitions with forbidden energy (eV) of argon after K-shell ionization

| Initial Configurations | | | Auger Transitions | E(ev) |
|---|---|---|---|---|
| i | j | k | | |
| 0 | 0 | 2 | $L_1L_2M_1$ | -7.13 |
| 0 | 0 | 2 | $L_1L_3M_2$ | -4.79 |
| 0 | 0 | 3 | $L_1L_2M_1$ | -24.12 |
| 0 | 0 | 3 | $L_1L_2M_2$ | -8.32 |
| 0 | 0 | 3 | $L_1L_2M_3$ | -8.02 |
| 0 | 0 | 3 | $L_1L_3M_1$ | -21.77 |
| 0 | 0 | 3 | $L_1L_3M_2$ | -5.97 |
| 0 | 0 | 3 | $L_1L_3M_3$ | -5.67 |
| 0 | 0 | 4 | $L_1L_2M_1$ | -42.30 |
| 0 | 0 | 4 | $L_1L_2M_2$ | -26.19 |
| 0 | 0 | 4 | $L_1L_2M_3$ | -25.87 |
| 0 | 0 | 4 | $L_1L_3M_1$ | -39.94 |
| 0 | 0 | 4 | $L_1L_3M_2$ | -23.83 |
| 0 | 0 | 4 | $L_1L_3M_3$ | -23.51 |
| 0 | 1 | 4 | $L_1L_2M_1$ | -61.84 |
| 0 | 1 | 4 | $L_1L_2M_2$ | -45.45 |
| 0 | 1 | 4 | $L_1L_2M_3$ | -45.10 |
| 0 | 1 | 4 | $L_1L_3M_1$ | -59.47 |
| 0 | 1 | 4 | $L_1L_3M_2$ | -43.08 |
| 0 | 1 | 4 | $L_1L_3M_3$ | -42.72 |
| 0 | 2 | 4 | $L_1L_2M_1$ | -83.00 |
| 0 | 2 | 4 | $L_1L_2M_2$ | -66.32 |
| 0 | 2 | 4 | $L_1L_2M_3$ | -80.61 |
| 0 | 2 | 4 | $L_1L_3M_1$ | -63.93 |
| 1 | 0 | 1 | $L_1L_2M_1$ | -14.11 |
| 1 | 0 | 1 | $L_1L_2M_1$ | -11.64 |
| 1 | 0 | 3 | $L_1L_3M_1$ | -31.62 |
| 1 | 0 | 3 | $L_1L_3M_3$ | -31.25 |

Figure 2 shows the Auger spectrum of selected lines after K shell ionization of Ar. The height of each bar is equal to the transition rates after K-shell ionization.

Auger transitions marked in brackets and the spectator vacancy configurations are in outside the brackets with each spectrum observed during the de-excitation cascades. The Auger satellite spectra appearing during the cascade development result from energy transitions that depend on the distribution of vacancies in the atomic configurations. These spectra are emitted in the presence of different configurations of additional vacancies left by preceding Auger transitions. The spectator vacancies change the screening of the electrons, thereby shifting the various partial spectra against each other. As shown in the figure, that the L spectator vacancy increases the Auger transition energy by view eV, whereas M spectator hole lowers the L-MM Auger transition energy by several eV.

Figure 3 shows the calculation of ion charge state distributions with and without consideration the energy forbidden transitions. It is found that, the forbidden of some low energy Auger transitions lead to increase the number of vacancies in the atom through the vacancy cascade development. The neglecting of the forbidden energy transitions in the calculations could change the successive of vacancy filling process that influences the results of ion charge state distributions. The de-excitation of core hole in Ar gives rise to different ionic charges. Each branch of the de-excitation leads to an ion of a specific charge. $Ar^{2+}$ ions are formed from $L_{23}$ hole and subsequent $L_{23}$-MM Auger transitions. The $L_{23}$ hole is generated after filling K-shell vacancy via $K_{\alpha}$ fluorescence. The K ionization followed by K-$L_{23}$M Auger transition leads to $Ar^{3+}$. The de-excitation pathway after K shell ionization is K-$L_{23}$M, $L_{23}$[M]-MM[M], this cascade leading to a stable $M^{-3}$ hole state ($Ar^{3+}$). The subsequent of K-$L_{23}L_{23}$ gives rise to final $Ar^{4+}$ ions. The de-excitation pathway of K shell hole is the successive K-$L_{23}L_{23}$, $L_{23}$[$L_{23}$]-MM[$L_{23}$], $L_{23}$[$M^2$]-MM[$M^2$]. $Ar^{5+}$ ions arise from subsequent K-$L_{23}L_{23}$ transition and from shake-off process. This process occurs from primary ionization and from Auger transitions in the course of de-excitation cascades. The electron shake-off process leads to additional holes in the outer shell of atom.

The de-excitation of K holes leads to production of $Ar^{n+}$ (n=4-6) ions. This hole transferred via K-$L_1L_1$ Auger transition, and subsequent $L_1$[$L_1$]-$L_{23}$M[$L_1$], $L_1$[$L_{23}$M]-$L_{23}$M [$L_{23}$M], $L_{23}$[$L_{23}M^2$]-MM[$L_{23}M^2$], $L_{23}$[$M^4$]-MM[$M^4$]. This branching gives rise to stable $M^{-6}$ hole state ($Ar^{6+}$). The consideration of Auger channels with forbidden energy in the course of de-excitation decays after K shell ionization leads to agreement results for ion charge state distributions with the experimental values.

**4- Conclusions**

The Auger spectra formed during vacancy cascade are calculated for certain Auger line of Ar atom after K shell ionization. The Auger transition rates and transition energies are obtained using Dirac- Fock -Slater wave functions. The influence of multi- vacancy that created through de-excitation cascades is considered in the calculation of ion charge states. The forbidden Auger channels due to the shift of binding energy levels are presented for L- Auger transitions. The Auger transition energy shifts in Ne and Ar atoms with several vacancies in the electronic configurations are calculated in the present work. The results for highly charged ions followed of K-shell ionization in Ar atom agree well with the experimental values.

## References


[1] R. K. Janev, L. Presnyakov: Phys. Rep. 70, (1981) 1107

[2] K. Ueda, E. Shigemasa, Y. Sato, S. Nagaoka, I. Koyano, A. Yagishita, T. Nagata and T. Hayaishi; Chem. Phys. Lett. 154 (1989) 357

[3] D. L. Matthews, B. M. Johnson, J. J. Mackey, and C. F. Moore; Phys. Rev. Lett. 31, (1973) 1331

[4] C. P. Bhalla, N. O. Folland, and M. A. Hein; Phys. Rev. A 8 (1973) 649.

[5] F. P. Larkins, J. Phys. B: At. Mol. Phys. 4 (1971) L29

[6] F. P. Larkins, J. Phys. B: At. Mol. Phys. 6 (1973) 2450

[7] M. N. Mirakhmedov; Nucl. Inst. and Methods Research B 98 (1995) 429

[8] M. N. Mirakhmedove; J. Phys. B: At. Mol. Opt. Phys. 21 (1988) 795

[9] A. M. El-Shemi, Y. A. Lotfy; European Physical J. D 31, (2005)

[10] A. M. El-Shemi; Jap. J. of App. Phys. 43 (2004) 2726

[11] A. M. El-Shemi; Canadian J. of Phys. 82 (2004) 811

[12] J. W. Cooper, S. H. Southworth, M. A. MacDonald, T. LeBrun; Phys. Rev. A 50, (1994) 405

[13] F. von Busch, J. Doppelfeld, C. Gunther and E. Hartmann; J. Phys. B: At. Mol. Opt. Phys. 27 (1994) 2151

[14] G. Omar, Y. hahn; Z. phys. D 25 (1992) 41

[15] M. Lorenz and E. Hartmann; Report ZFI-109, Leipzig, 27 (1985)

[16] I. P. Grant, B. J. Mckenzie, P. Norrington, D. F. Mayers, and N. C. Pyper; Comput. Commun. 21 (1980) 207

[17] T. A. Carlson, M. O. Krause, and W. H. Johnston; Phys. Rev. 133 (1964) A385
[18] D. A. Church, S. D. Kravis, I. A. Sellin, J. C. Levin, R. T. Short, M. Meron, B. M. Johnson, and K. W. Jones; J. Phys. B 25 (1992) 121

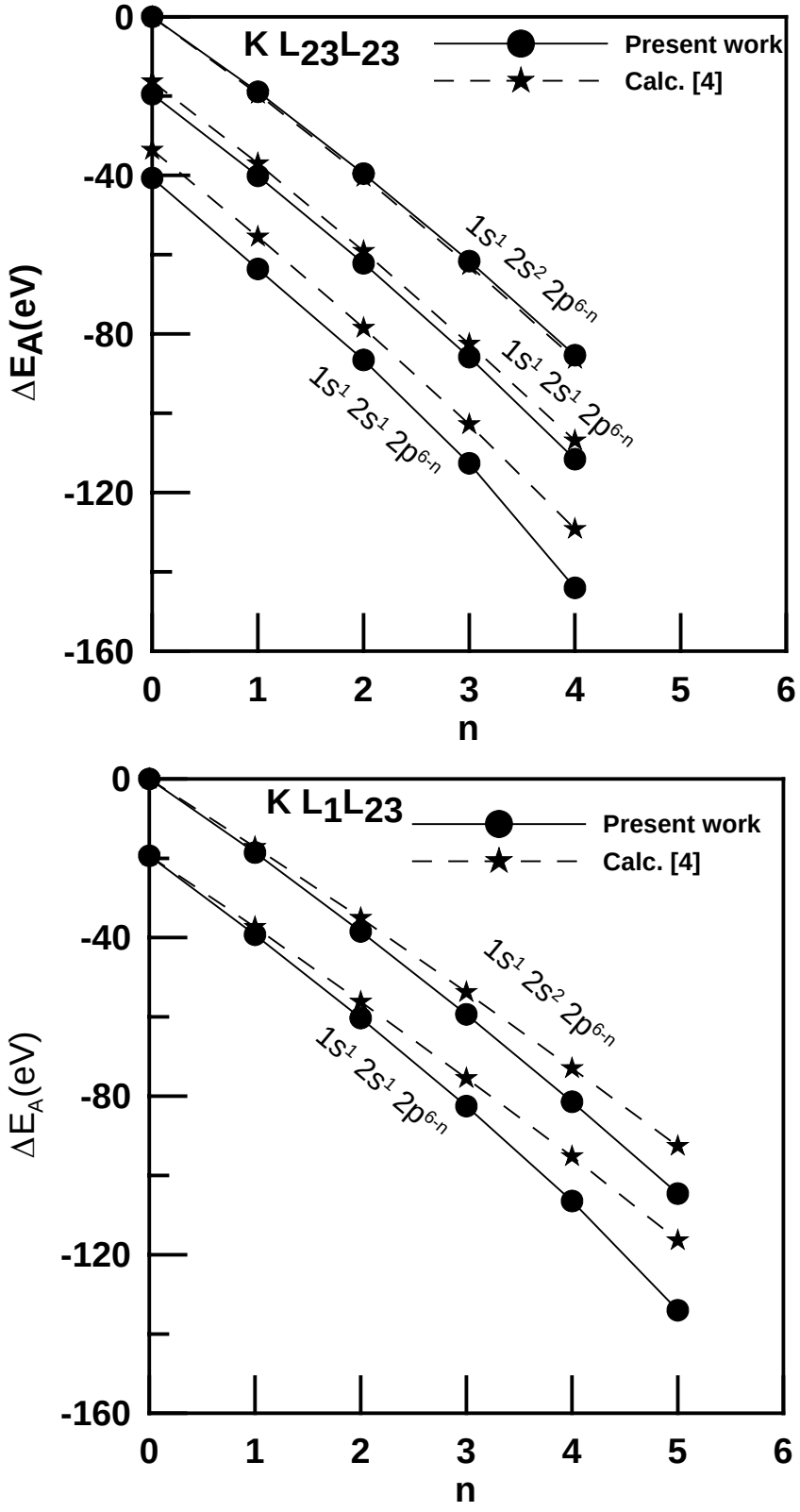


Figure 1: The shifts of Auger electron energy of multi-ionized Ne

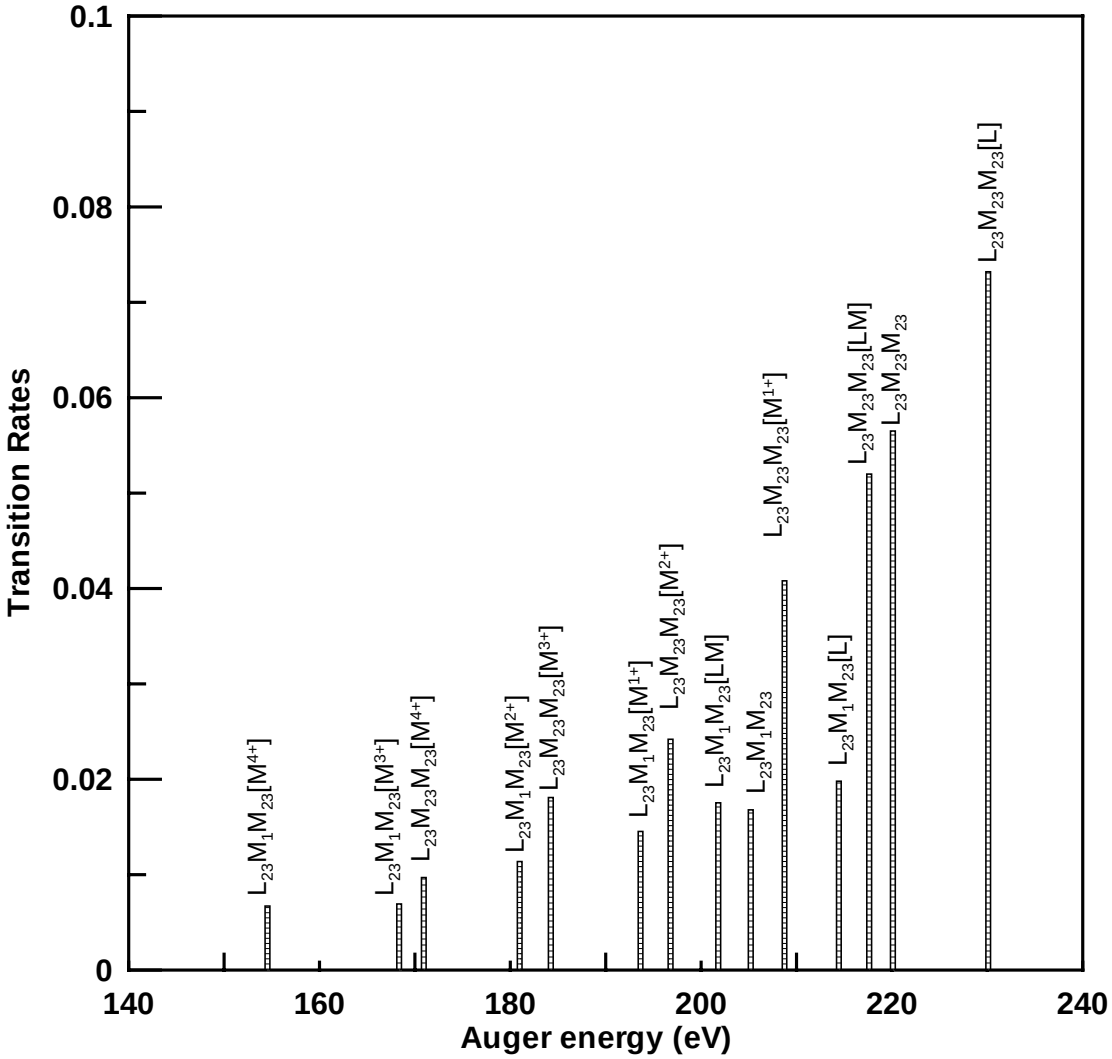


Figure 2: The Auger spectrum for selected lines after K-shell ionization in Ar atom

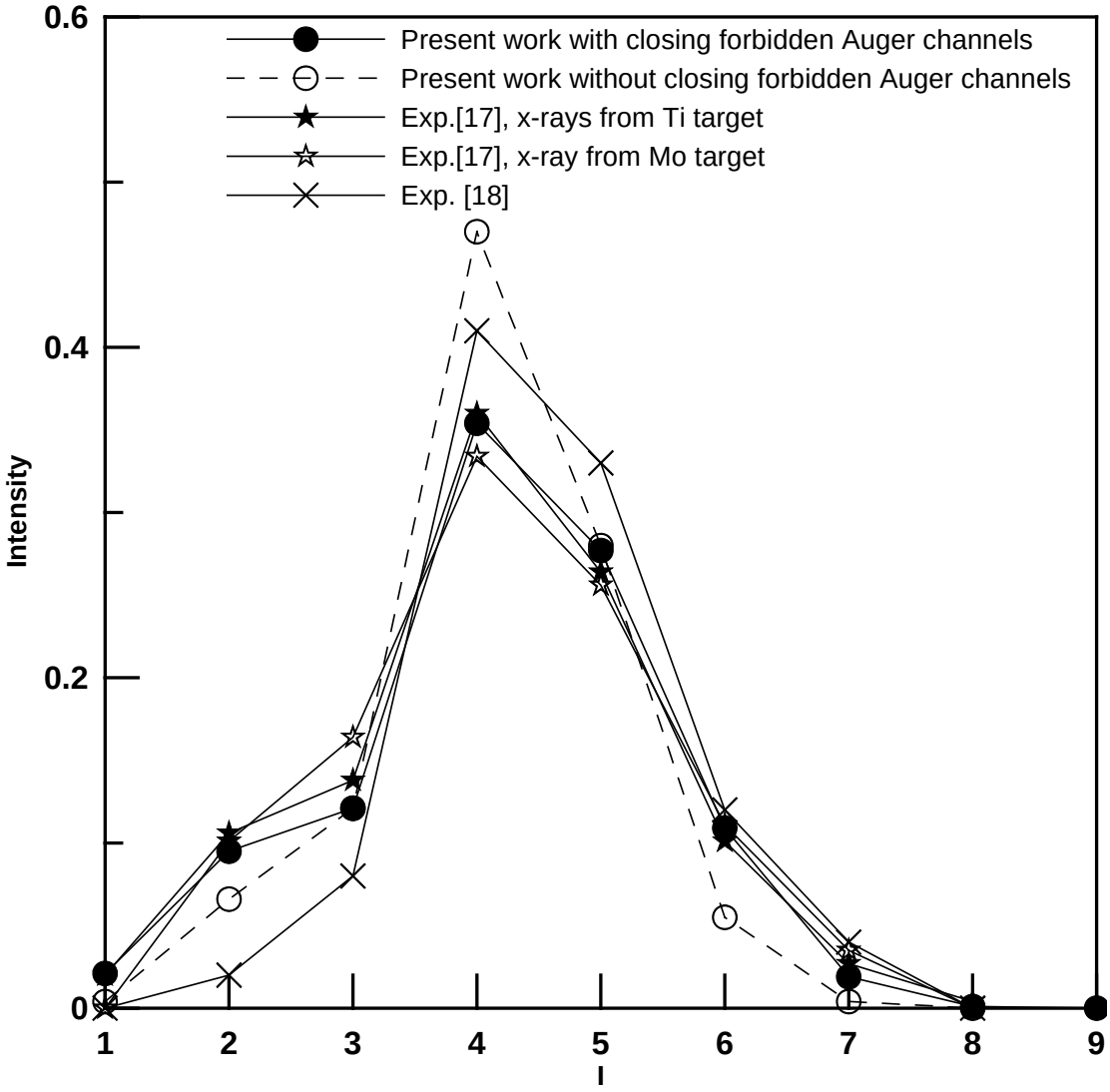


Figure 3: Charge state of ions produced after K- ionization in Ar